International Scientific Conference 20 UNITECH 26

INTERNATIONAL SCIENTIFIC CONFERENCE
19-21 November 2026
GABROVO

COOLING-RATE DEPENDENCE OF THE ATOMIC STRUCTURAL EVOLUTION OF CERIUM DURING RAPID SOLIDIFICATION

Murat Celtek[1], Unal Domekeli[2]

[1]*Faculty of Education, Trakya University, 22030, Edirne – Türkiye*
[2]*Dept. of Physics, Trakya University, 22030, Edirne – Türkiye*

……

**Corresponding author: mceltek@trakya.edu.tr and muratceltek@gmail.com*

Abstract

In this study, the effect of cooling rate on the atomic structure of cerium during the rapid solidification process was investigated using classical molecular dynamics (MD) simulations. The open-source LAMMPS package was chosen for the atomic simulations, and the embedded atom method (EAM) was used to model atomic interactions. The initial cerium structure was generated in the γ-fcc phase in the simulations, and the cooling process was carried out at four different rates. The structural evolution of cerium during heating and cooling processes was analyzed using the temperature dependence of potential energy, the pair distribution function, and the common neighbor analysis method performed via OVITO. The analysis results revealed that the selected EAM potential successfully predicted the structural properties of solid and liquid cerium. Additionally, the results showed that the cooling rate significantly affected the microstructural evolution of cerium. In conclusion, this simulation is expected to provide valuable data to guide future studies investigating the microstructural and mechanical responses of cerium systems under boundary conditions.

Keywords: cerium, molecular dynamics, embedded atom method, pair distribution function, common neighbor analysis, cooling rate.

INTRODUCTION

The localization of f-electrons, which is characteristic of rare-earth elements, forms the basis of many functional industrial applications, including permanent magnets, phosphors, and magnetostrictive systems [1, 2]. Cerium (Ce) is one of the most remarkable examples in this group. It exhibits rare phase behavior in materials science, which is characterized by an isostructural transition between two face-centered cubic (fcc) phases, α and γ. This behavior also includes a minimum point on the melting curve and a solid-solid critical point that terminates at approximately 550 K and 1.9 GPa [3–5]. Due to its striking similarities in crystal structure, melting temperature, and phase transition behavior, Ce is considered a reliable, nonradioactive surrogate for delta-plutonium (δ-Pu) alloys in nuclear studies [6, 7]. Although there are numerous studies in the literature on the phase behaviors and transformations of Ce, research focusing on its atomic evolution during rapid solidification processes and the effects of cooling rate on microstructure is quite limited. The study presented aimed to address this gap by comprehensively investigating the atomic behavior of Ce, which possesses an initial γ-fcc structure, during heating and rapid solidification processes using classical molecular dynamics (MD) simulations. In simulations conducted using the LAMMPS software and the embedded-atom method (EAM) potential, the effects of different cooling rates on potential energy (PE) change, the pair distribution function (g(*r*)), and

This is an open access article licensed under Creative Commons Attribution 4.0 International
Print ISSN: 1313-230X, Online ISSN: 3033-1404

common neighbor analysis (CNA) were quantitatively determined. These findings are expected to guide future research on the dynamic, structural, and mechanical responses of Ce systems under extreme conditions.

EXPOSITION

The EAM potential, widely used in metallic systems, represents the many-body character of metallic bonding by accounting for the embedding energy of each atom within the local electron density, in addition to pairwise interatomic interactions. This approach provides a suitable framework for investigating structural evolution processes, such as solid-liquid transformations and solidification, by accounting for changes in the local atomic environment and coordination. Accordingly, the general mathematical expression that defines the total energy of the EAM potential used in the study is given by Equation (1) [8, 9].

$$E_T = \frac{1}{2}\sum_{i,j,i\neq j}^{N}\varphi_{ij}(r_{ij}) + \sum_{i}^{N}F_i(\rho_i), \qquad (1)$$

where $\varphi_{ij}(r_{ij})$ represents the interatomic pair interaction term and $F_i(\rho_i)$ represents the embedding energy of the *i*-th atom, which depends on its local electron density (ρ_i).

MD simulations of pure Ce were performed using the LAMMPS software [10] package with the EAM potential [11]. The system was initially constructed with a 4,000 atom fcc structure. Newton's equations of motion were integrated using a 1 fs time step and the leapfrog algorithm. All simulations were performed using the NPT ensemble. The system temperature was controlled using a Nosé-Hoover thermostat [12, 13], while the pressure was fixed at P=0 GPa with the aid of a barostat. The system was heated from 200 K to 1650 K at a rate of 0.33 K/ps in 50 K increments. Then, it was cooled back down to 200 K in 50 K increments at four different cooling rates (20, 5, 1 and 0.33 K/ps).

The exact agreement between the lattice parameter (5.16 Å) and cohesive energy (4.32 eV/atom) values calculated via EAM-MD and the experimental data from Kittel [14](a_0 = 5.16 Å and E_{coh} = 4.32 eV/atom) confirms that the employed interaction potential accurately describes the Ce system's fundamental crystallographic and thermodynamic properties and validates the reliability of the simulation results.

Fig. 1 shows the potential energy-temperature (PE-T) variations for the solidification processes of Ce at a heating rate of 0.33 K/ps and different cooling rates, including 0.33, 1, 5, and 20 K/ps. During the heating process, the system's PE energy exhibits an approximately linear increase with temperature in the 200–1350 K range. On the other hand, observing a distinct and sudden increase in PE within the 1350–1400 K range suggests that a significant rearrangement of the atomic structure of the system occurs within this temperature range. When evaluated alongside subsequent structural analyses, this abrupt change can be attributed to the transition of Ce from the solid phase to the liquid phase. The melting temperature of 1350 K predicted by EAM-MD simulations for γ-Ce is approximately 25.9% higher than the experimental value. This difference shows that the potential can represent the solid-liquid transition and melting behavior of Ce in a physically meaningful manner, despite potential quantitative deviations arising from the nature of the EAM potential employed and the classical MD approach. In the liquid phase above the melting point and during the initial stages of supercooled, the PE curves for all cooling rates overlap completely, indicating that the system remains in equilibrium independent of the cooling rate within the high-temperature regime, where atomic mobility is high. During slow cooling (0.33 to 1 K/ps), crystallization occurs, accompanied by a sudden drop in energy between 550 and 650 K. This occurs because the atoms have time to settle into a stable lattice. Conversely, during rapid cooling (5 to 20 K/ps), this sudden drop is completely

suppressed. This freezes the liquid structure, yielding a glassy or amorphous (metallic glass) phase.

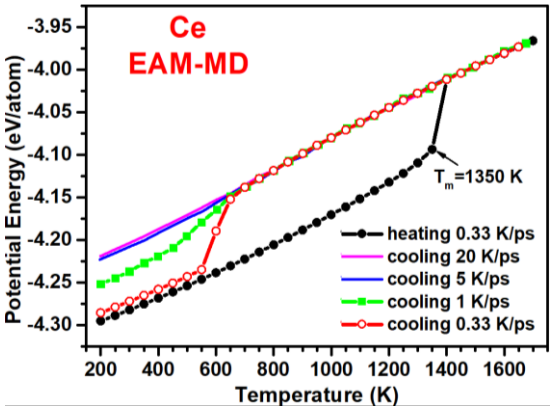


Fig. 1. *Comparison of the PE-T curves of Ce during cooling and heating.*

g(*r*) is the most fundamental and powerful structural analysis tool that directly reveals atomic packing, local order, and phase transformations in amorphous and crystalline structures. For more information on the theoretical details of atomic-scale changes during the solidification process and g(*r*) analysis, please refer to the relevant literature [15–19]. Figs. 2(a–c) depict the g(*r*) curves, which were calculated to investigate the evolution of the atomic-scale structure as a function of temperature and cooling rate. In simulations performed at a high cooling rate of 5 K/ps (Fig. 2(a)), a characteristic splitting of the secondary peak was observed as the temperature dropped from 1600 K to 300 K, which is a well-known hallmark of amorphous structures and metallic glasses [20–23]. However, sharp crystalline peaks indicative of long-range order did not form, and the system retained its amorphous, glassy structure. At a cooling rate of 0.33 K/ps (Fig. 2(b)), it is observed that the g(*r*) curves exhibit more distinct and sharp peaks particularly below 600 K unlike those observed at other cooling rates. These peaks became more pronounced as the temperature decreased, providing strong evidence for the development of long-range atomic order associated with crystallization. Fig. 2(c) shows a temperature-dependent comparison of different cooling rates. It reveals that at temperatures above 1000 K, the structure retains its liquid character regardless of the cooling rate. Conversely, at room temperature (300 K), decreasing the cooling rate from 20 K/ps to 0.33 K/ps leads to a significant increase in peak intensity and gradual rise in structural order. In this process, a cooling rate of 1 K/ps emerges as an intermediate regime that exhibits transitional characteristics between the high-speed amorphous state (5–20 K/ps) and the distinct crystalline phase (0.33 K/ps). The increase in peak amplitudes observed at 300 K represents an intermediate structural phase in which the system begins to exhibit a tendency toward crystallization.

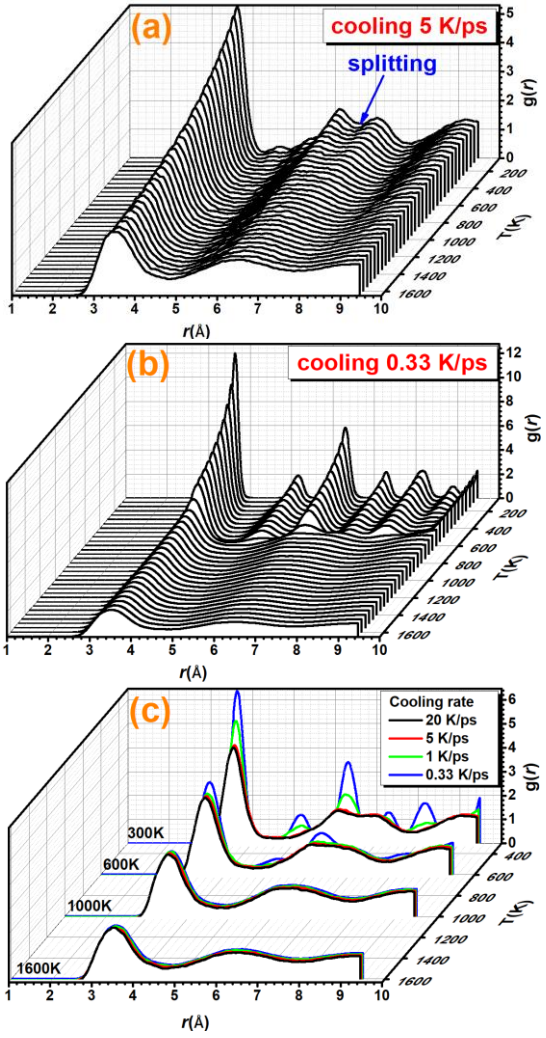


Fig. 2*. Temperature-dependent evolution of g(r) for the Ce melt at different cooling rates: (a) glass formation at 5 K/ps, (b) crystallization at 0.33 K/ps, and (c) comparison of g(r) curves for four cooling rates at temperatures of 1600 K, 1000 K, 600 K, and 300 K.*

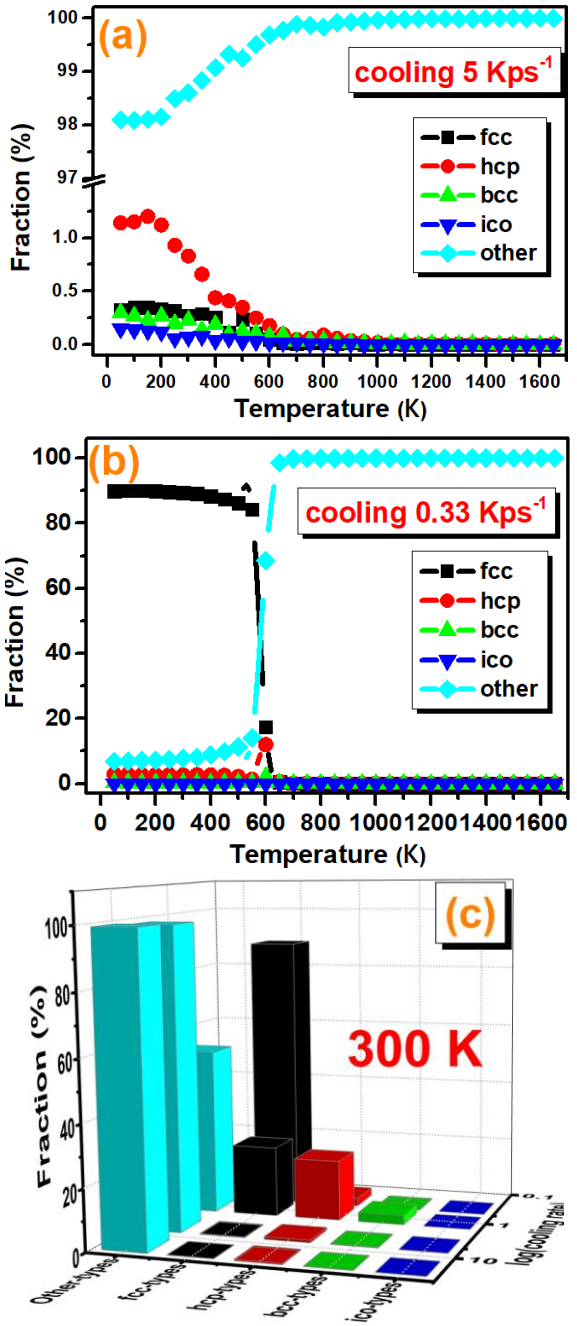


Fig. 3. *Temperature-dependent evolution of the system's CNA analysis results at cooling rates of (a) 5 K/ps and (b) 0.33 K/ps, and (c) CNA results at 300 K for all cooling rates.*

Fig. 3(a) shows the CNA results at a cooling rate of 5 K/ps. As the figure shows, the high cooling rate did not allow the atoms sufficient time to diffuse into stable lattice positions. This prevented nucleation and caused the system to remain highly disordered (98%-100%) and solidify into an amorphous/glassy structure. By contrast, the system that solidified at a cooling rate of 0.33 K/s experienced rapid nucleation and crystallization at a critical transformation temperature of around 600 K. As shown in Fig. 3(b), during the slow cooling process, the amorphous atom fraction decreased rapidly, while the thermodynamically preferred fcc phase became dominant, exceeding 90% at room temperature.

The small amount (5%-10%) of the hcp phase observed in the structure is associated with stacking faults and twin boundaries within the fcc matrix. In conclusion, the 3D column analyses (Fig. 3(c)) summarizing the dependence of the phase distribution at 300 K on the cooling rate confirm that the critical cooling rate threshold for the amorphous-to-crystalline transformation in the system lies between the high and low cooling regimes investigated.

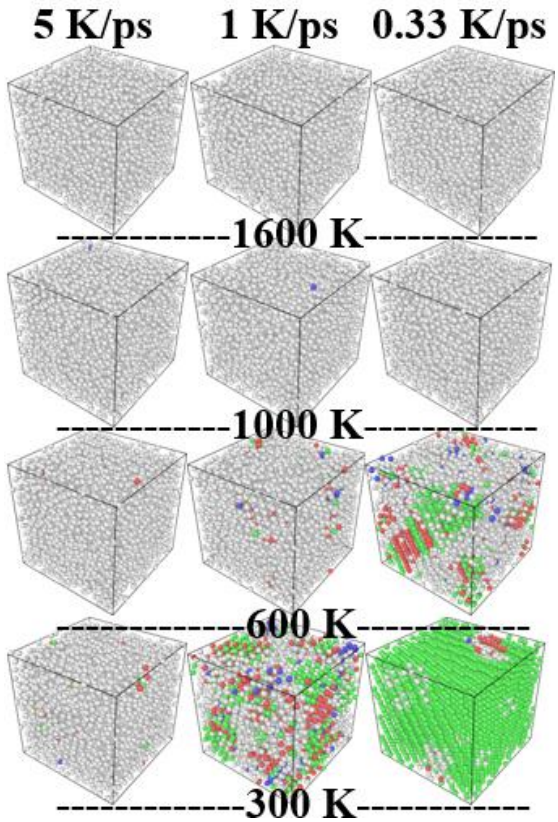


Fig. 4. *Snapshots of atomic configurations of Ce melt obtained at different cooling rates and temperatures (Green: fcc, Red:hcp, Blue: bcc, Transparent/Gray: Liquid/Amorphous).*

Fig. 4 shows snapshots of local atomic structures as determined by CNA analysis and visualized using the OVITO package

[24]. As can be seen in the images, it is clear that the disordered liquid structure at 1600 K transforms into an amorphous phase at a high cooling rate (5 K/ps) without significant nucleation when cooled to 300 K. In contrast, at the lowest cooling rate of 0.33 K/ps, fcc (green) nuclei are observed to grow rapidly within the matrix, particularly starting from a temperature of 600 K. At 300 K, the structure consists almost entirely of an ordered fcc phase with hcp (red) layers representing stacking faults dispersed within it. With a cooling rate of 1 K/s, partial crystal nucleation was observed at 600 K and 300 K. This confirms that the system is at the boundary of the amorphous-to-crystalline transition and represents the critical cooling threshold.

The results of all analyses indicate that the cooling rate significantly influences the solidification process, the phases formed, and the final atomic structure of the system.

CONCLUSION

In this study, the rapid solidification behavior of Ce and the changes in its atomic structure depending on the cooling rate have been investigated in detail using EAM-based MD simulations. The main results obtained are presented below:

i. The EAM potential predicted the lattice parameter and cohesive energy of γ-Ce to be 5.16 Å and 4.32 eV/atom, respectively. These values show excellent agreement with the experimental results reported in the literature. In addition, the melting temperature of the system was determined to be 1350 K using EAM-MD. Although the calculated value is slightly higher than the experimental melting temperature, the results indicate that the solid-liquid transition of Ce can be reasonably described by the EAM potential employed.

ii. The PE-T and g(r) results demonstrated that the cooling rate has a significant effect on solidification behavior. At high cooling rates (5–20 K/ps), nucleation was largely suppressed, and the system remained stable in a glassy structure at low temperatures. This structure was also evidenced by the splitting of the second peak in the g(*r*) function.

iii. At a cooling rate of 0.33 K/ps, crystallization occurred at around 600 K according to all analysis results. CNA analyses and 3D atomic structure images showed that the fcc structure became dominant at 300 K, making up more than 90% of the total structure.

iv. With a cooling rate of 1 K/ps, a mixed structure with a transition between glassy and crystalline regions was obtained. This suggests that the system did not completely crystallize and that different local structural arrangements coexist.

The results obtained reveal that the cooling rate is one of the key parameters that determine the solidification behavior and final atomic structure of Ce. These results also provide an important reference for future studies that aim to understand the rapid solidification processes of rare-earth metals at the atomic scale.

REFERENCE

[1] GschneidnerJr KA, Pecharsky VK, Tsokol AO. Recent developments in magnetocaloric materials. Reports Prog Phys 2005; 68: 1479–1539.

[2] Coey JMD. Permanent magnets: Plugging the gap. Scr Mater 2012; 67: 524–529.

[3] Johansson B. The α-γ transition in cerium is a Mott transition. Philos Mag 1974; 30: 469–482.

[4] Lawson AW, Tang T-Y. Concerning the High Pressure Allotropic Modification of Cerium. Phys Rev 1949; 76: 301–302.

[5] Dupont V, Chen S-P, Germann TC. Isomorphic phase transformation in shocked Cerium using molecular dynamics. EPJ Web Conf 2010; 10: 00009.

[6] Boehlert CJ, Farr JD, Schulze RK, et al. Initial electron back-scattered diffraction observations of cerium. Philos Mag 2003;

83: 1735–1744.
[7] Zhao K, Gu Y, Zhao F, et al. Revisiting the effect of shear stress on the γ→α phase transition of cerium under shock loading. Mech Mater 2023; 184: 104743.
[8] Daw MS, Baskes MI. Embedded-atom method: Derivation and application to impurities, surfaces, and other defects in metals. Phys Rev B 1984; 29: 6443–6453.
[9] Celtek M, Domekeli U, Sengul S, et al. Effects of Ag or Al addition to CuZr-based metallic alloys on glass formation and structural evolution: a molecular dynamics simulation study. Intermetallics 2021; 128: 107023.
[10] Plimpton S. Fast Parallel Algorithms for Short-Range Molecular Dynamics. J Comput Phys 1995; 117: 1–19.
[11] Sheng HW. EAM potentials, https://sites.google.com/site/eampotentials/ce-trivalent?authuser=0 (2026).
[12] Nosé S. A unified formulation of the constant temperature molecular dynamics methods. J Chem Phys 1984; 81: 511–519.
[13] Hoover WG. Canonical dynamics: Equilibrium phase-space distributions. Phys Rev A 1985; 31: 1695–1697.
[14] Kittel C. *Introduction to Solid State Physics*. New York: John Wiley & Sons Inc., 1986.
[15] Guder V, Celtek M, Celik FA, et al. Crystallization analysis and determination of Avrami exponents during isothermal annealing and the effect of cooling rate on the evolution of the atomic structure of Pd78Si16Cu6 alloy: A molecular dynamics simulation study. J Non Cryst Solids 2023; 602: 122067.
[16] Celtek M, Domekeli U, Sengul S. Strontıum Under High Pressure and Different Temperature Conditions: A Molecular Dynamics Simulation Study. In: *International Scientific Conference*. Gabrovo-Bulgaria, 2022, pp. 328–332.
[17] Domekeli U, Celtek M. Melting Mechanism Of Cylindrical Molybdenum Nanowire: A Molecular Dynamics Simulation Study. In: *Unitech – Selected Papers*. Gabrovo-Bulgaria, 2024. Epub ahead of print 2024. DOI: 10.70456/LPWG1883.
[18] Domekeli U. A molecular dynamic study of the effects of high pressure on the structure formation of liquid metallic Ti62Cu38 alloy during rapid solidification. Comput Mater Sci 2021; 187: 110089.
[19] Domekeli U, Celtek M. A Molecular Dynamics Simulation Study of the Melting and Solidification Processes of Hafnium Nanoparticles. Langmuir 2026; 42: 28003–28016.
[20] Celtek M, Sengul S, Domekeli U, et al. Molecular dynamics simulations of glass formation, structural evolution and diffusivity of the Pd-Si alloys during the rapid solidification process. J Mol Liq 2023; 372: 121163.
[21] Celtek M, Sengül S, Domekeli U. The Evolution of Atomic Structure of the Zr48Cu36Ag8Al8 Bulk Metallic Glass in the Rapid Cooling Process. Süleyman Demirel Univ J Nat Appl Sci 2019; 23: 954–962.
[22] Celtek M. In-depth investigation of the effect of cooling rate on structural and dynamic properties of Cu54Hf46 alloy by molecular dynamics simulations. J Non Cryst Solids 2025; 664: 123615.
[23] Celik FA. Cooling rate dependence of the icosahedral order of amorphous CuNi alloy: A molecular dynamics simulation. Vacuum 2013; 97: 30–35.
[24] Stukowski A. Visualization and analysis of atomistic simulation data with OVITO-the Open Visualization Tool. Model Simul Mater Sci Eng 2010; 18: 015012.